2.5A DEVELOPMENT OF A NEW PARAMETERIZATION FOR REPRESENTING BOUNDARY LAYER CLOUDS IN MESOSCALE MODELS

Jean-Christophe Golaz[1] *, Vincent E. Larson[2], and William R. Cotton[1]
[1]Dept. of Atmospheric Science, Colorado State University, Fort Collins, Colorado.
[2]Dept. of Mathematical Sciences, University of Wisconsin, Milwaukee, Wisconsin.

1. INTRODUCTION

Boundary layer clouds play an important role in the energy and water cycles, both on a regional and global scale. The incorporation of such clouds in present-day numerical models continues to pose a significant challenge. The parameterization of these clouds is commonly seen as a multiplicity of tasks, including predicting heat and moisture fluxes, cloud cover, and cloud water. To compute these quantities, many parameterizations use multiple schemes and are then faced with the difficult problem of interfacing the various schemes and ensuring consistency among them.

An alternative viewpoint is that the above tasks can be seen as parts of a single job: the prediction of the joint probability density function (PDF) of vertical velocity, heat and moisture content. Atmospheric PDFs vary with time and space and contain a wealth of information. In particular, given the joint PDF, the subgrid heat and moisture fluxes, cloud cover, and liquid water can all be diagnosed in a unified manner. Predicting the full PDF is not computationally feasible, but we can assume a functional form for the PDF. The problem then reduces to the selection of a particular member from the family of PDFs for each grid box and time step.

PDFs have been used to parameterize subgrid-scale moisture variations as a way to account for partial cloud cover by Manton and Cotton (1977), Sommeria and Deardorff (1977), Bougeault (1981a), and Chen and Cotton (1987). Randall *et al.* (1992) outlined a bulk second order closure scheme making use of a double-delta PDF to represent turbulent moments. Lappen and Randall (2001a,b,c) developed a scheme unifying a higher-order closure with a mass-flux approach.

A new PDF-based parameterization is presented here. This single parameterization is intended to model a variety of boundary layer cloud types in a unified framework. The representation of the subgrid scale PDF is based on analysis of aircraft observations and high resolution model outputs (Larson *et al.* 2001). Results show that a proper choice for the family of PDFs can lead to a unified framework capable of simulating a wide range of cloudiness regimes.

*Corresponding author address: Jean-Christophe Golaz, Dept. of Atmospheric Science, Colorado State University, Fort Collins, Colorado 80523; e-mail: golaz@atmos.colostate.edu.

2. MODEL DESCRIPTION

The PDF methodology can be outlined as follows. One first writes down standard higher-order moment equations based on the Navier-Stokes equations. This includes prognostic equations for second-order moments and the third order moment of the vertical velocity. These moments are then used to select a particular member from the family of PDFs. Once the PDF is fixed, unclosed higher-order moments can be computed and cloud fraction and cloud water diagnosed.

The parameterization is implemented in a single-column framework and is integrated in time and space. During a model time step, the PDF approach can be summarized in three major steps:

(i) Predict mean quantities and higher-order turbulent moments.

(ii) Use the predicted moments to select the PDF for a particular model grid box and time step.

(iii) Close higher-order moments and diagnose cloud fraction and cloud water using the PDF.

In traditional closure models, higher-order moments are often closed using a down-gradient or a quasi-normal assumption which can be poor assumptions for cumulus layers. The PDF approach differs in the sense that once the representation of the PDF is determined, unclosed moments, cloud fraction and cloud water can all be diagnosed in a consistent manner.

2.1 Basic equations

The basic variables used in the single-column model are the horizontal winds $\overline{u}$ and $\overline{v}$, the liquid water potential temperature $\overline{\theta_l}$, and the total specific water content $\overline{q_t}$. The mean vertical velocity $\overline{w}$ is imposed. Predictive equations for these variables are the traditional Reynolds averaged equations, where $\overline{\psi}$ denotes horizontal averages and ψ' perturbations from the mean (e.g. Stull 1988):

$$\frac{\partial \bar{u}}{\partial t} = -\bar{w}\frac{\partial \bar{u}}{\partial z} - f(v_g - \bar{v}) - \frac{\partial}{\partial z}\overline{u'w'} \tag{1}$$

$$\frac{\partial \bar{v}}{\partial t} = -\bar{w}\frac{\partial \bar{v}}{\partial z} + f(u_g - \bar{u}) - \frac{\partial}{\partial z}\overline{v'w'} \tag{2}$$

$$\frac{\partial \bar{q}_t}{\partial t} = -\bar{w}\frac{\partial \bar{q}_t}{\partial z} - \frac{\partial}{\partial z}\overline{w'q_t'} \tag{3}$$

$$\frac{\partial \bar{\theta}_l}{\partial t} = -\bar{w}\frac{\partial \bar{\theta}_l}{\partial z} - \frac{\partial}{\partial z}\overline{w'\theta_l'} - \bar{R} \tag{4}$$

where $\bar{R}$ is the radiative heating rate, u_g, v_g are the geostrophic winds, and f is the Coriolis parameter.

In addition to these four basic variables, the model predicts seven higher-order moments used for the description of the subgrid-scale PDF: $\overline{w'^2}$, $\overline{w'^3}$, $\overline{q_t'^2}$, $\overline{\theta_l'^2}$, $\overline{q_t'\theta_l'}$, $\overline{w'q_t'}$, $\overline{w'\theta_l'}$. The prognostic equations for the higher-order moments are similar to Bougeault (1981b) with the exception that the quasi-normal approximation has not been used to close the fourth order moment ($\overline{w'^4}$) appearing in the $\overline{w'^3}$ equation. These equations also contain unclosed third order moments as well as buoyancy terms. The momentum fluxes $\overline{u'w'}$ and $\overline{v'w'}$ are closed using a down-gradient approach.

2.2 Description of the PDF

A good candidate for the representation of the subgrid-scale variations of w, θ_l, and q_t was found to be a double-Gaussian with correlation between θ_l and q_t within each Gaussian hump (Larson *et. al* 2001):

$$G(w', \theta_l', q_t') = aG_1(w', \theta_l', q_t') + (1-a)G_2(w', \theta_l', q_t') \quad (5)$$

where $G_i(w', \theta_l', q_t')$

$$\begin{aligned} &= \frac{1}{(2\pi)^{3/2}\,\sigma_{wi}\,\sigma_{q_{ti}}\,\sigma_{\theta_{li}}\,(1-r^2_{q_t\theta_l})^{1/2}} \\ &\times \exp\left\{-\frac{1}{2}\left(\frac{w'-(w_i-\bar{w})}{\sigma_{wi}}\right)^2\right\} \\ &\times \exp\left\{-\frac{1}{2(1-r^2_{q_t\theta_l})}\left[\left(\frac{q_t'-(q_{ti}-\bar{q}_t)}{\sigma_{q_{ti}}}\right)^2+\left(\frac{\theta_l'-(\theta_{li}-\bar{\theta}_l)}{\sigma_{\theta_{li}}}\right)^2\right.\right. \\ &\qquad \left.\left. - 2r_{q_t\theta_l}\left(\frac{q_t'-(q_{ti}-\bar{q}_t)}{\sigma_{q_{ti}}}\right)\left(\frac{\theta_l'-(\theta_{li}-\bar{\theta}_l)}{\sigma_{\theta_{li}}}\right)\right]\right\} \end{aligned}$$

This family of PDFs depends on a number of free parameters:

- a: relative weight of the first Gaussian.
- $\psi 1, \psi 2, \sigma_{\psi 1}, \sigma_{\psi 2}$: locations and widths of the vertical velocity (w), liquid water potential temperature (θ_l), and total specific water content (q_t) Gaussians.
- $r_{q_t\theta_l}$: intra-Gaussian correlation between liquid water potential temperature and total specific water content.

These parameters can be computed analytically from the mean quantities and higher-order moments predicted by the model to yield a complete description of the subgrid-scale PDF. Because the model does not predict the skewness of θ_l and q_t, we make the simplifying assumption that they are proportional to the skewness of w.

2.3 PDF closure

Once the PDF free parameters have been determined, the PDF is integrated to close all remaining unclosed higher-order moments and diagnose cloud fraction and water. As an example, the fourth order moment of w can be expressed in terms of the PDF free parameters using:

$$\begin{aligned} &\overline{w'^4} \qquad (6) \\ &= \int_{-\infty}^{\infty}\int_{-\infty}^{\infty}\int_{-\infty}^{\infty} w'^4\, G(w', \theta_l', q_t')\, dw'\, d\theta_l'\, dq_t' \\ &= a\left((w_1-\overline{w})^4 + 6(w_1-\overline{w})^2\sigma_{w1}^2 + 3\sigma_{w1}^4\right) \\ &\quad +(1-a)\left((w_2-\overline{w})^4 + 6(w_2-\overline{w})^2\sigma_{w2}^2 + 3\sigma_{w2}^4\right) \end{aligned}$$

3. RESULTS

The parameterization was tested on cases selected to represent a wide range of conditions, including a clear convective boundary layer, maritime and continental cumulus layers, and a stratocumulus layer. To allow for a detailed evaluation of the parameterization, three-dimensional simulations of all cases were performed using the Regional Atmospheric Modeling System (RAMS) (Pielke *et. al* 1992) in its large-eddy simulation (LES) configuration. Results from three cases are presented:

- **BOMEX**. Trade-wind cumulus cloud layer based on the 4th GCSS (GEWEX Cloud Study System) intercomparison workshop.
- **ARM**. Cumulus clouds over land forming on top of an initially clear convective layer. This case is based on the 6th GCSS intercomparison workshop.
- **FIRE**. Nocturnal stratocumulus deck idealized from measurements taken during the FIRE experiment off the coast of California. This case is based on the First GCSS intercomparison workshop. (Moeng *et al.* 1996, Bechtold *et al.* 1996)

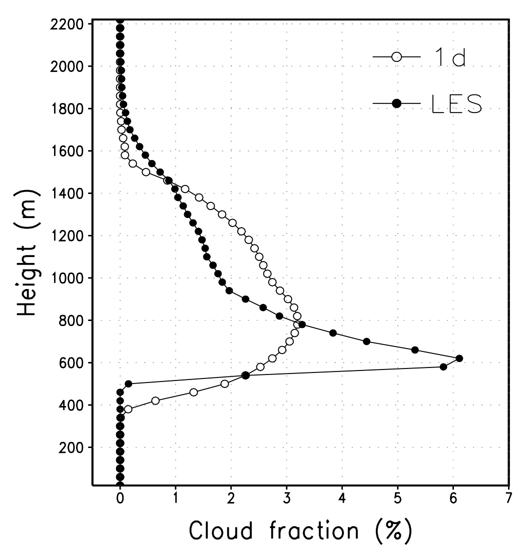

Figure 1: Vertical profiles of cloud fraction for the BOMEX case using the single-column model and the LES. Averaged over the last hour of simulation.

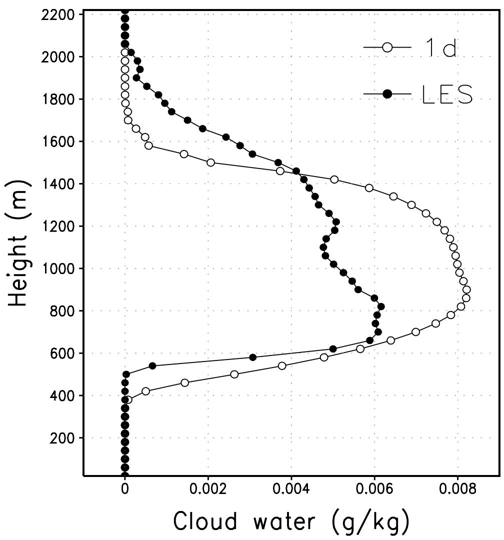

Figure 2: Same as Figure 1 but for cloud water.

Simulation lengths, vertical grid spacings, and main time steps for all the three cases are shown in Table 1.

Experiment	Simulation Length (hours)	Vertical Grid Spacing (m)	Time Step (s)
BOMEX	6	40	20
ARM	14.5	40	20
FIRE	3	25	6

Table 1: Simulation time, vertical grid spacing and main time step for the single-column model for each test case.

3.1 BOMEX

For the trade-wind cumulus case based on BOMEX, the single-column model produces a 3.5% maximum cloud fraction. After an initial burst in convection during the first hour, it produces a nearly steady-state cloud fraction profile with no intermittency.

Profiles comparing the cloud fraction between the single-column model and the LES are shown in Figure 1. The overall agreement is good given the very small amount of cloud cover. The LES results show a maximum value of cloud fraction near cloud base of approximately 6%. This maximum is not fully captured by the single-column model. Cloud base is underestimated by approximately 100 (m), and so is cloud top, although by a larger amount.

Comparison of the cloud water specific content is shown in Figure 2. The amount of condensate is approximately 30% larger in the single-column model than in the LES in the lower part of the cloud layer. For comparison purposes, results from the GCSS intercomparison workshop showed that most single-column models predicted cloud water amounts that were typically five to ten times larger than the LESs (www.knmi.nl/~siebesma/gcss/bomex.html). The unified mass-flux scheme of Lappen and Randall (2001b,c) also produces a cloud water content that is approximately eight times larger than the LES.

3.2 ARM

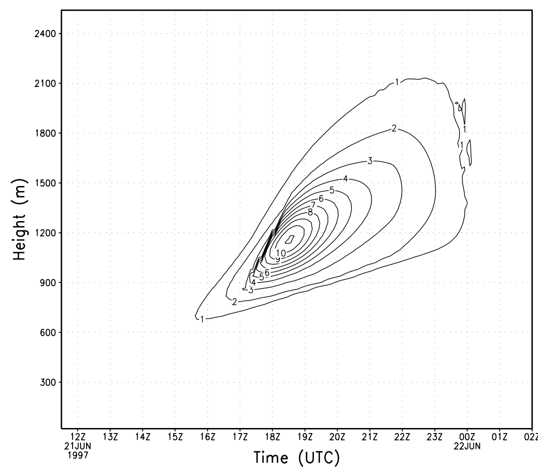

Figure 3: Time evolution of cloud fraction using the single-column model for the ARM case.

The time evolution of the cloud fraction obtained with the single-column model for the ARM case is shown in Figure 3. Cumulus clouds form on top of a previously clear convective boundary layer and deepen during the course of the day. The maximum cloud fraction reached is approximately 11%. The first clouds appear around 1600 UTC and the last ones dissipate after 0000 UTC. The timing of the onset and decay of clouds is similar between the parameterization and the LES where clouds are present between 1530 UTC and 0020 UTC.

Mean profiles of cloud fraction for the parameterization and the LES are depicted in Figure 4. The LES exhibits a maximum cloud fraction of 11.5% near cloud base, compared to 8.5% for the single-column model. The shape of the vertical profile is comparable between the two models, but cloud fraction decreases faster with height in the parameterization than it does in the LES, leading to an underestimation of cloud top. This problem is likely to be caused by the assumption of proportionality between the skewnesses of vertical velocity and total water. Although reasonable in the middle part of the cloud layer, this assumption becomes questionable in the upper part. A model predicting skewness of total water could potentially remedy this shortcoming. Values of cloud water (not shown) are slightly smaller in the single-column model as compared to the LES.

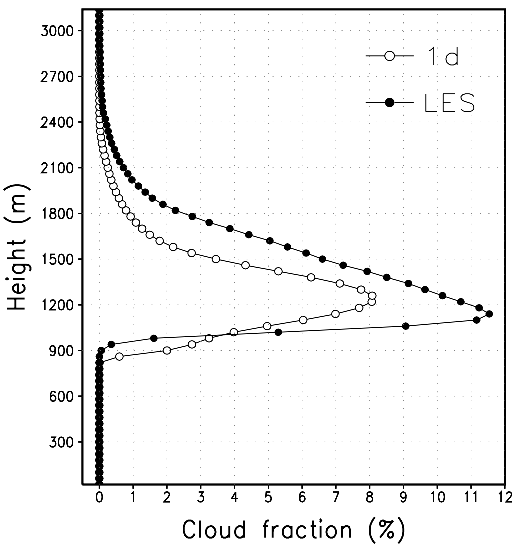

Figure 4: Vertical profiles of cloud fraction for the ARM case using the single-column model and the LES. Averaged between 1900 and 2000 UTC.

3.3 FIRE

The last case presented consists of a simulation of a nocturnal solid stratocumulus deck. Profiles of cloud cover obtained with the parameterization and the reference LES are shown in Figure 5. They are nearly identical except for a vertical displacement, with the single-column model producing a cloud cover that is approximately 50 meters lower than the one from the LES.

Profiles of cloud water specific content shown in Figure 6 exhibit larger differences. The single-column model produces a maximum cloud water amount of 0.15 g/kg compared to 0.25 g/kg for the LES. This difference can possibly be explained by the fact that the parameterization produces mean profiles of θ_l and q_t that are not nearly as well-mixed as in the LES (not shown). This leads to a slightly smoother inversion in the single-column model and a smaller amount of total water specific content below the inversion near cloud top, possibly resulting in the observed reduction in liquid water.

4. CONCLUSION

A new boundary layer clouds parameterization is described. It utilizes a family of joint PDFs for representing the subgrid-scale variability of vertical velocity, heat, and moisture content. The form of the PDF chosen is based on analysis of aircraft observations and high resolution model outputs of cloudy boundary layers. The PDF representation forms the basis of a new turbulence closure scheme that can be used to compute all higher-order terms needed as well as diagnose cloud fraction, cloud water and buoyancy related moments, all in a manner consistent with the PDF.

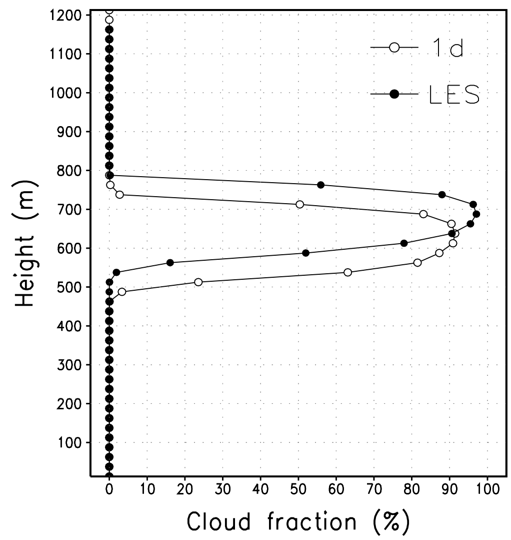

Figure 5: Vertical profiles of cloud fraction for the FIRE case using the single-column model and the LES. Averaged over the last hour of the simulation.

Three different test cases consisting of a trade-wind cumulus layer, cumulus clouds over land, and a nocturnal stratocumulus layer were presented. The comparison with the reference LESs was generally good. The parameterization was capable of simulating cumulus boundary layer clouds with low cloud fraction and cloud water amounts. With no adjustment, the same scheme was also found to be able to produce high cloud cover as evidenced by the simulation of a nocturnal stratocumulus deck.

These results demonstrate the strength of the PDF parameterization approach: given a family of PDFs sufficiently flexible and general, it is possible to construct a unified scheme capable of successfully simulating very different boundary layer cloudiness regimes.

5. REFERENCES

Bechtold, P., S. K. Krueger, W. S. Lewellen, E. van Meijgaard, C.-H. Moeng, D. A. Randall, A. van Ulden, and S. Wang, 1996: Modeling a stratocumulus-topped PBL: intercomparison among different one-dimensional codes and with large eddy simulation. *Bulletin of the American Meteorological Society,* **77,** 2033-2042.

Bougeault, Ph., 1981a: Modeling the trade-wind cumulus boundary layer. Part I: Testing the ensemble cloud relations against numerical data. *Journal of the Atmospheric Sciences.* **38,** 2414-2428.

Bougeault, Ph., 1981b: Modeling the trade-wind cumulus boundary layer. Part II: A higher-order one-dimensional model. *Journal of the Atmospheric Sciences.* **38,** 2429-2439.

Chen, C. and W. R. Cotton, 1987: The physics of the marine stratocumulus-capped mixed layer. *Journal of the Atmospheric Sciences.* **44,** 2951-2977.

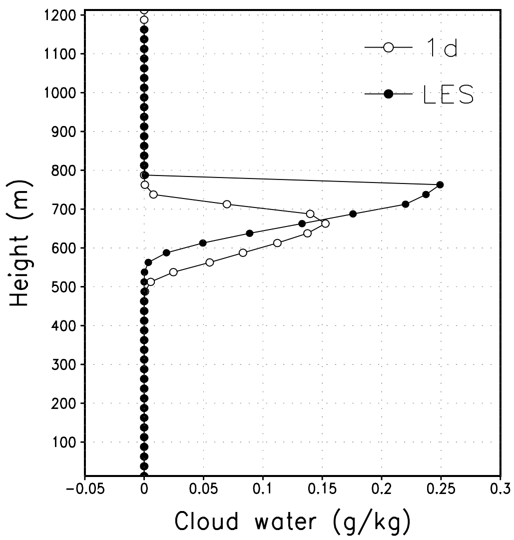

Figure 6: Same as Figure 5 but for cloud water.

Lappen, C.-L. and D. A. Randall, 2001a: Towards a unified parameterization of the boundary layer and moist convection. Part 1: A new type of mass-flux model. *Journal of the Atmospheric Sciences.* In Press.

Lappen, C.-L. and D. A. Randall, 2001b: Towards a unified parameterization of the boundary layer and moist convection. Part 2: Lateral mass exchanges and subplume-scale fluxes. *Journal of the Atmospheric Sciences.* In Press.

Lappen, C.-L. and D. A. Randall, 2001c: Towards a unified parameterization of the boundary layer and moist convection. Part 3: Simulations of clear and cloudy convection. *Journal of the Atmospheric Sciences.* In Press.

Larson, V. E., J-Ch. Golaz, Robert Wood, Paul R. Field, Thomas H. Vonder Haar, and W. R. Cotton, 2001: Parameterizing boundary layer clouds using PDF methods. Ninth Conference on Mesoscale Processes, Ft. Lauderdale, Florida. **P1.17A**.

Manton, M. J., and W. R. Cotton, 1977: Formulation of approximate equations for modeling moist deep convection on the mesoscale. Atmospheric Science Paper Number 266, Fort Collins, Colorado, 62pp.

Moeng, C.-H., W. R. Cotton, C. Bretherton, A. Chlond, M. Khairoutdinov, S. Krueger, W. S. Lewellen, M. K. MacVean, J. R. M. Pasquier, H.A. Rand, A. P. Siebesma, B. Stevens, and R. I. Sykes, 1996: Simulation of a stratocumulus-topped planetary boundary layer: intercomparison among different numerical codes. *Bulletin of the American Meteorological Society,* **77,** 261-278.

Pielke, R. A., W. R. Cotton, R. L. Walko, C. J. Tremback, W. A. Lyons, L. D. Grasso, M. E. Nicholls, M. D. Moran, D. A. Wesley, T. J. Lee, and J. H. Copeland, 1992: A comprehensive meteorological modeling system RAMS. *Meteorology and Atmospheric Physics,* **49**, 69-91.

Randall, D. A., Q. Shao, and C.-H. Moeng, 1992: A second-order bulk boundary-layer model. *Journal of the Atmospheric Sciences.* **49,** 1903-1923.

Stull, R. B., 1988: An Introduction to Boundary Layer Meteorology. Kluwer Academic, 666pp.

Sommeria, G. and J. W. Deardorff, 1977: Subgrid-scale condensation in models of non-precipitating clouds. *Journal of the Atmospheric Sciences.* **34,** 344-355.